Modified Bertaut Method to Determine Cation Distribution and Valence State in Powders of Spinels Through X-ray Diffraction

Jose Alonso Hernandez de la Cruz and Pierre Giovanni Mani Gonzalez *

Posted Date: 12 January 2024

doi: 10.20944/preprints202401.0980.v1

Keywords: XRD; spinels; vacancies; optimization; cation distribution

Article

Modified Bertaut Method to Determine Cation Distribution and Valence State in Powders of Spinels through X-ray Diffraction

José Alonso Hernández de la Cruz and Pierre Giovanni Mani-González *

Department of Physics and Mathematics, Institute of Engineering and Technology, Universidad Autónoma de Ciudad Juárez, Av del Charro 450 Col. Partido Romero, C.P. 32310, Juárez, Chihuahua, México.

* Correspondence: pierre.mani@uacj.mx

Abstract: In this work a new method is proposed to tackle down the multiple objective optimization problem of the calculation of cation distribution in spinels structure, through the difference of intensity ratios between experimental and calculated intensities of cation sensitive Bragg planes, by introducing a new factor, $R_{abs,}$ in Bertaut method. This factor is introduced as the sum of absolute R factors, and it is minimized by varying cation distribution. To test this method aluminate manganese spinel where synthesized though modified Pechini method and characterized though XRD. The results show to be in agreement with literature for the aluminum inversion in tetrahedral sites, which is near to the reported value of 10%. Also, it was noticed that the manganese atoms are present in octahedral sites with a mixed valence state of +2 and +3. Which might be an indicator that oxygen vacancies are present in the structure, so the vacancies value of oxygen is proposed considering the total charge of cations and thus proposing the value of 3.678 mol per formula unit of the spinel, thus having the next stoichiometry considering normalized Al and Mn, $MnAl_2O_{3.678.}$ Finally, the last cation distribution proposed was $\left[Mn^{+2}_{0.867}Al^{+3}_{0.129}\right]\left[Mn^{+2}_{0.034}Mn^{+3}_{0.098}Al^{+3}_{1.871}\right]O_{3.678}$ with a R_{abs} factor value of 0.6466, which considers the cation distribution and oxygen vacancies.

Keywords: XRD; spinels; vacancies; optimization; cation distribution

Introduction

Spinel structure has as general chemical formula AB_2X_4. Where A atoms are elements with +2 valence state, B atoms are elements with +3 valence state and X is usually oxygen or a chalcogenide such as sulfur. In last case, spinels are named thiospinels. The order of cations in A and B sites sometimes has an inversion of atoms occupation site. It means in A site (tetrahedral site) +3 valence state atoms and in B site (octahedral site) +2 valence state atoms. Suggesting an inverse spinel. [1–4].

Some spinels have an intermediate distribution of cations between A and B site as mixed spinel. It is the most common state for even normal spinels. The ordering of the cations in the spinel structure directly determines the behavior of its optical, electrical, magnetic, thermal, and chemical properties. Thus, it is important to determine the inversion spinel degree [3–7].

Transition metals have usually more than one allowed valence state, such as Mn that can have up to 7 valence states. Since the valence state also affects the properties of the spinel, it is fundamental to estimate the average valence state when present mixed spinels. By intensity ratios of X-Ray diffraction planes sensitive to cation distribution; which is an easiest and more reliable technique rather than neutron diffraction, Mossbauer spectroscopy or X-Ray photoelectron spectroscopy [8–11].

Recently we have been studying aluminum manganese spinels, for the purpose of using it as a cathode material in aluminum ion batteries. In batteries one aspect that might dictate the electrochemical behavior of the spinel in the electrochemical cell is the cation distribution of the atoms in the structure since a redox couple and the valence of the transition metals tends to change to lower or higher average valence. Then, to study the cation distribution of these spinels we developed a

Preprints (www.preprints.org) | NOT PEER-REVIEWED | Posted: 12 January 2024 doi:10.20944/preprints202401.0980.v1

more accurate method to approximate the cation distribution based on the works of *Bertaut et al, Ashish and Hiren, Siva Ram Prasad et al* and *Lakhani et al.* [3,9,12].

Manganese aluminate spinels are a class of materials that have the chemical and structural formula AB_2O_4, thus crystallize in the same structure as $MnAl_2O_4$. It holds the space group No 227 $FD\bar{3}M$ with Mn atom occupying A site with a valence of +2 and Al atoms occupying B site with a valence of +3. (See Supplementary Information Figure SI1) Although this spinel is pointed out to be a normal spinel it tends to show a small degree of inversion as pointed by *Stokes et al,* with a value of inversion of i=0.1, where also it has been found that the Mn atoms in B site have +2 and +3 valence states showing an average valence state higher than expected and that depends on the method of synthesis. [9,13]

The atomic coordinates for this spinel vary depending on the origin choice for the space group $FD\bar{3}M$. Two different equipoints with point symmetries $\bar{4}3m$ and $\bar{3}m$ are possible origins for the unit cell. Thus, having the next Wyckoff positions for the atoms for each origin setpoint, see Table 1.[14]

Table 1. Wyckoff positions of atoms for the two possible origin choice for space group 227.

Origin Choice	Wyckoff Positions		
	Al	**Mn**	**O**
1	8a	16b	32e
2	8b	16c	32e

Considering the multiple valence state that manganese can have, it has been pointed out by *Stokes et al* that the general cation distribution formula for this spinel could be $\left[Mn^{+2}_{1-(i+x)}Al^{+3}_{i}\right][Mn^{+2}_{i}Mn^{+3}_{x}Al^{+3}_{1-i}]O_4$.[9]

Methodology

Synthesis of Manganese Aluminate Spinels

The synthesis was performed by the modified Pechini method which involves making a solution in a beaker with deionized water and the metal chloride salts of Al and Mn in stochiometric quantity according to target stoichiometry. To this solution was added ethylene glycol and was stirred under heat to 50°C for 20 min. Citric acid was added as complexing agent in molar relation to salts of 3:1 and the solution was heated to 150°C for 5 h for polyesterification reaction. After gelation this was taken to an oven at 200°C for 3 h to dry the gel. Following a calcination step at 1100°C for 2 h with a heating curve of 20°C/min.[15–17]

X-Ray diffraction intensity

For the determination of cation distribution, it is considered the ratios of the intensity between sensitive planes to cation distribution such as (220), (400), (422) and (440). (220) and (422) planes are sensitive to cation distribution in A site, while (400) and (440) planes are sensitive to both A and B site cation distribution, as evidenced *Vara Prasad et al.* The reason to consider ratios of planes intensity rather than individual intensities is because ratios of intensity allow to avoid crystal preferential orientations in powder samples.[1]

The most important value to determinate the intensity planes ratios, is the relative intensity for each individual plane, thus the formula for calculating the intensity of diffraction for a determined plane can be expressed as equation 1.[18]

$$I_{hkl} = |F_{hkl}|^2 \cdot p \cdot L_p \qquad \textit{Equation 1}$$

Where, I_{hkl} is the relative integrated intensity, F_{hkl} is the structure factor, p is the multiplicity factor (see Table 3) and L_p is the Lorentz polarization factor (see equation 7)

Preprints (www.preprints.org) | NOT PEER-REVIEWED | Posted: 12 January 2024 doi:10.20944/preprints202401.0980.v1

Structure Factor

The structure factor is calculated considering the atomic scattering factor. The atomic scattering factor is used to describe the efficiency of scattering of the atoms in a given direction, so it is defined as a ratio of amplitudes, see equation 2.

$$F = \frac{amplitude\ of\ a\ wave\ scattered\ by\ an\ atom}{amplitude\ of\ a\ wave\ scattered\ by\ an\ electron} \qquad Equation\ 2$$

Atomic scattering factor depends on the Bragg angle and the wavelength of incident beam. The calculation of *f* involves $sin\,\theta$ rather than the value of θ, due to the net effect is that *f* decreases as quantity $\frac{\sin\theta}{\lambda}$ increases. The scattering factor *f* is sometimes called the form factor because it depends on the way in which of electrons are distributed around the nucleus at the atom. The resultant wave scattered by all atoms in the unit cell is called the structure factor because it describes how the atom arrangement affects the scattered beam. Thus, the structure factor, designated by the symbol *F*, is obtained adding together all the waves scattered by individual atoms. If a unit cell contains atoms 1, 2, 3…N, with fractional coordinates $u_1\,v_1\,w_1$, $u_2\,v_2\,w_2$, $u_3\,v_3\,w_3$… and atomic scattering factors f_1, f_2, f_3…, then the structure factor for a *hkl* reflection is given by equation 3, [5,12,18]

$$F_{hkl} = \sum_1^N f_n e^{2\pi i(hu_n+kv_n+lw_n)} \qquad Equation\ 3$$

Then, the structure factors equations for the Bragg planes, as stated by *Ashish and Hiren,* in the spinel structure are the ones shown in Table 2.[12]

Table 2. Structure factors for special Bragg planes of spinel structure.

Bragg´s Planes	Structure Factor
(220)	$-8F_A$
(311)	$4(-\sqrt{2}F_A - 2F_B)$
(400)	$8(-F_A+2F_B+4F_O)$
(422)	$8F_A$
(440)	$8(F_A+2F_B+4F_O)$

Where F_A and F_B are structure factors for A site and B site cations and F_O oxygen site.

The atomic form factor for each atom in each plane, which is employed in the structure factor as a consequent of Bragg plane determination; it is multiplied by the occupation in the site by the correspond atom and adding this factor for each atom present in the site. The atomic form factor is the Fourier transform of the electron density per atom; it is assumed a spherically symmetric electron density, its values of the Fourier transform only depend on the distance from the origin of the reciprocal space. It is approximated by a sum of Gaussians. (See equation 4)

$$f\left(\left|\vec{G}\right|\right) = \sum_{i=1}^{4} a_i e^{\left(-b_i\left(\frac{G}{4\pi}\right)^2\right)} \qquad Equation\ 4$$

Where vector $\frac{G}{4\pi}$ equals $\frac{\sin\theta}{\lambda}$ and the sum can be computed for factors a_i and b_i from coefficients computed by *Mann and Cromer.* (See supplementary information Table SI1)[19]

Multiplicity Factor (p)

The relative proportion of planes that contribute to the same reflection enter on the intensity equation as the magnitude *p* may be defined as the number of different planes in the same spacing. The value of *p* as a function of *hkl* are given below in Table 3.[18]

Table 3. Multiplicity factors for special Bragg planes for spinel structure.

Bragg´s Planes	Multiplicity Factors
(220)	12
(311)	24
(400)	6

Preprints (www.preprints.org) | NOT PEER-REVIEWED | Posted: 12 January 2024 doi:10.20944/preprints202401.0980.v1

(422)	24
(440)	24

Lorentz Polarization Factor (L_p)

Considering trigonometrical factors that influence on the intensity of the reflected beam helps to calculated a polarization and Lorentz corrections to remove its effect from the relative intensity of Bragg peaks and background. (See equations 5 and 6)

$$Lorentz\ Factor = \left(\frac{\cos\theta}{(\sin 2\theta)^2}\right) \qquad \textit{Equation 5}$$

$$Polarization\ Factor = P(\theta,\gamma) \cong \frac{1+(\cos 2\theta)^2}{2} \qquad \textit{Equation 6}$$

Then, both equations get combined to obtain a single Lorentz-Polarization factor that is expressed as shown in equation 7.[18]

$$Lorentz - Polarization\ Factor = L_p = \frac{1+(\cos 2\theta)^2}{(\sin\theta)^2\cos\theta} \qquad \textit{Equation 7}$$

Method

Usually when the method of intensity ratios for sensible planes to cation distribution is employed; a mapping of the concentration of cations in each side is done, where a changes in cation normal to be at B site is done by 5% step down to a 50% changes in concentration at A site. Then the cation distribution that gives the closest value to 0 for each R factor of each intensity ratios between experimental and calculated, is looked minimal for the four ratios. [1,3,12] The problem with it is the time consumed looking for the lowest R factor for the four ratios, and another problem is that by considering more elements and valence states in the system the permutations increase exponentially making more difficult to analyze the cation distribution of the system.

Since, the nature of this problem is a multiple objective optimization; we proposed a new factor R_{abs} which is the sum of all absolute R factors difference of each intensity ratios between experimental and calculated intensities. (See equation 8)

$$R_{abs} = \left|R_{\frac{400}{220}}\right| + \left|R_{\frac{400}{422}}\right| + \left|R_{\frac{440}{422}}\right| + \left|R_{\frac{440}{220}}\right| \qquad \textit{Equation 8}$$

Where,

$$R_{\frac{400}{220}} = \frac{I_{exp}400}{I_{exp}220} - \frac{I_{cal}400}{I_{cal}220} \qquad \textit{Equation 9}$$

$$R_{\frac{400}{422}} = \frac{I_{exp}400}{I_{exp}422} - \frac{I_{cal}400}{I_{cal}422} \qquad \textit{Equation 10}$$

$$R_{\frac{440}{422}} = \frac{I_{exp}440}{I_{exp}422} - \frac{I_{cal}440}{I_{cal}422} \qquad \textit{Equation 11}$$

$$R_{\frac{440}{220}} = \frac{I_{exp}440}{I_{exp}220} - \frac{I_{cal}440}{I_{cal}220} \qquad \textit{Equation 12}$$

The reason to take the absolute value of the equations 9,10, 11 and 12 is the fact that sometimes with some cation distributions the difference will have some values that are negative but may be also a minimum. So, to take the closest value of R to 0 we have to consider only the distance from 0 no matter if it is positive or negative; then making sure that we have the global minima and not a local minimum. For example, if we consider a value of R_1=-0.5 and R_2=1; the value that is closest to 0 is -0.5 (See Figure 1)

Preprints (www.preprints.org) | NOT PEER-REVIEWED | Posted: 12 January 2024 doi:10.20944/preprints202401.0980.v1

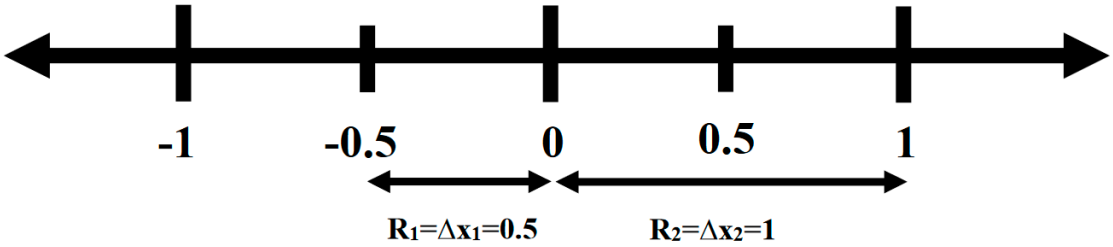

Figure 1. R factor values range and their relative distance to 0.

Thus, by employing this new equation we can make this multiple objective optimization problem a single objective optimization, where we want to optimize R_{abs} to 0; which would be when no difference is present between ratios.

The solution for this single objective optimization was tackled down with the algorithm evolutionary solver. In which a minimization target was set, and the next constraints were set $Al^{+3}{}_{B\ site} \leq 2$, $Al^{+3}{}_{B\ site} >= 1$, $Mn^{+2}{}_{B\ site} <= 1$, $Mn^{+2}{}_{B\ site} >= 0$, Occupancy of B site should be 2.

1. *Characterization XRD*

The X-Ray diffraction patterns were acquired in a X´pert Pro Panalytical system with a Cu Kα X-Ray source with a wavelength of 1.541 Å, with a 2Θ range from 10° up to 70° with a step of 0.016° at 298.19 K under air.

2. *I_{obs}/I_{cal} Method*

The proposed method was applied to manganese aluminate spinels and the next 2Θ and intensity for the Bragg planes were acquired through the experimental XRD characterization of the spinel. (See Table 4)

Table 4. position and relative intensity of Bragg planes.

Bragg Planes	2Θ(°)	Relative Intensity
(220)	31.64	45.55
(311)	37.32	100
(400)	43.43	46.55
(422)	54.46	17.96
(440)	64.02	59.37

The X-Ray diffraction pattern was normalized to highest intensity Bragg plane (311). (See Figure 2)

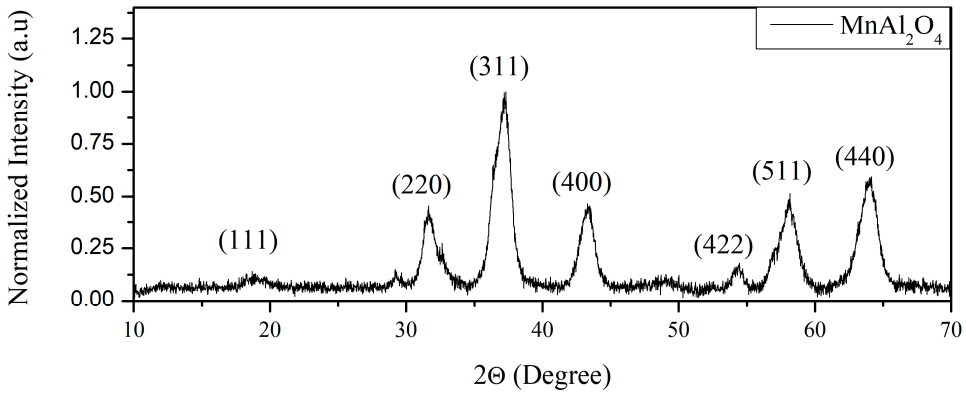

Figure 2. X ray diffraction pattern of synthesized manganese aluminate spinel.

Preprints (www.preprints.org) | NOT PEER-REVIEWED | Posted: 12 January 2024 doi:10.20944/preprints202401.0980.v1

Average valence state

The average valence state of the transition metal in the structure of the spinel was calculated by adding the concentration of +2 valence in both sites A and B site and the same procedure for +3 valence. Then it was multiplied by the concentration of each valence on both sites.

Results

The modified Bertaut method described is shows in Table 5. Where three cases were optimized in order to determine the valence state of the cations in the spinel structure of manganese aluminate spinel. Since *Stokes et al.* have made the statement that this spinel shows two valence states for the occupation of Mn in B site, which is with valences +2 and +3. So, to test the method an optimization was calculated where only Mn^{+2} was considered in B site, which is shows in the first 3 rows of Table 5. It can be pointed out that it has agreement between R factors due to the individual R factor is less than 1, R_{abs}=0.6548. Also, can be pointed out that an inversion is shows where aluminum is presents in A site in an occupancy of 0.136, which is really agreement to the reported by *Stokes et al and Pierre Villars.*[9,20]

The second case tested where only Mn^{+3} was allowed to be in B site, is shows in Table 5 rows 4 to 6. In the value of R_{abs} has increased its values to 0.6832 suggesting that even though +3 is the valence of the site B, it means some manganese +2 might be in the site since the Mn^{+2} only allowed case showed a smaller R_{abs} value than this case.

Finally, the third case where a mixed valence between Mn^{+2} and Mn^{+3} is taking in account and as expected it showed the lowest value of R_{abs}. This inversion degree for aluminum is near to reported values of 10% in A site. Also, the preference of manganese for A site although it can also be present in B site with a mixed valence, but preferably with the valence of +3 since it is the valence of the site. It has the highest occupancy of manganese in the site B. The still difference between experimental and calculated, meaning the R factors are attributed to the fact that no absorption and Debye-Weller temperature factor were taken in account for the calculation. Since it has been shown that the effect of these factors is small against the cation distribution.[1]

Table 5. Cation distribution, R factors and Rabs factor for each case where a) considers only Mn+2 b) considers only Mn+3 and c) considers both Mn +2 and +3.

a)

Site A		Site B			400/220			400/422			440/422			440/220			Rabs
Al+3	Mn+2	Al+3	Mn+3	Mn+2	Obs	Cal	R	Obs	Cal	R	Obs	Cal	R	Obs	Cal	R	
0.1359	0.8626	1.864	0	0.1374	1.022	1.201	0.179	2.592	3.061	0.469	3.306	3.305	5E-04	1.303	1.297	0.007	0.6548

b)

Site A		Site B			400/220			400/422			440/422			440/220			Rabs
Al+3	Mn+2	Al+3	Mn+3	Mn+2	Obs	Cal	R	Obs	Cal	R	Obs	Cal	R	Obs	Cal	R	
0.074	0.924	1.926	0.076	0	1.022	1.025	0.003	2.592	2.626	0.034	3.306	2.851	0.455	1.303	1.113	0.191	0.6832

c)

Site A		Site B			400/220			400/422			440/422			440/220			Rabs
Al+3	Mn+2	Al+3	Mn+3	Mn+2	Obs	Cal	R	Obs	Cal	R	Obs	Cal	R	Obs	Cal	R	
0.1289	0.8672	1.871	0.0985	0.0344	1.022	1.19	0.168	2.592	3.035	0.444	3.306	3.286	0.02	1.303	1.288	0.015	0.6466

The final cation distribution proposed for this sample is the one shown below.

$$[Mn^{+2}_{0.867}Al^{+3}_{0.129}][Mn^{+2}_{0.034}Mn^{+3}_{0.098}Al^{+3}_{1.871}]O_4$$

The analysis of the total charge of the cations in the structure, it has a value of positive 7.356; in the ideal structure the oxygen should be 4 atoms per formula unit, meaning a negative charge of -8. Thus, since the electric charge of the structure must be equals to oxygen the difference can be explained as a deficiency in oxygen meaning the structure might have vacancies of oxygen, thus the final proposed cation distribution considering oxygen vacancies as shown below.

$$[Mn^{+2}_{0.867}Al^{+3}_{0.129}][Mn^{+2}_{0.034}Mn^{+3}_{0.098}Al^{+3}_{1.871}]O_{3.678}$$

Now that a final cation distribution is achieved, the total charge of manganese can be calculated and that would be the average valence of manganese which is an important value for applications

such as batteries, where it is important to know the average valence of an atom that works in the redox couple of the battery. The average valence of the manganese in this structure is 2.098.

Conclusion

Aluminum manganese spinel was synthetized through the modified Pechini method. Cation distribution was estimated though comparing experimental and calculated X-Ray diffraction intensity ratios of cation sensitive Bragg planes. Afterwards, the average valence of manganese in the structure was calculated. The proposed cation distribution showed an inversion of 12.9% in tetrahedral site for aluminum. Also, the manganese showed to be presents in the octahedral sites and being present in two valence states +2 and +3, which suggests an indication that some oxygen deficiency in the structure is presents. This vacancy was calculated resulting 3.678 mol instead of 4 mol of oxygen per formula unit. These results prove that this method is a robust powerful tool to determine of cation distribution in spinels accurately and with mixed valence in its cations. Achieving similar results for this system as found in literature. In future the absorbance and temperature Debye-Weller factor will be introduced in the method to reduce the R_{abs} value.

Acknowledge: Author´s would like to thanks to PRODEP-UACJ for supporting funds.

References

1. B. Vara Prasad, B. Rajesh Babu, and M. Siva Ram Prasad, "Structural and dielectric studies of Mg 2+ substituted Ni-Zn ferrite," *Mater. Sci.*, vol. 33, no. 4, pp. 806–815, 2015, doi: 10.1515/msp-2015-0111.
2. M. Siva Ram Prasad, B. B. V. S. V. Prasad, B. Rajesh, K. H. Rao, and K. V. Ramesh, "Magnetic properties and DC electrical resistivity studies on cadmium substituted nickel–zinc ferrite system," *J. Magn. Magn. Mater.*, vol. 323, no. 16, pp. 2115–2121, Aug. 2011, doi: 10.1016/J.JMMM.2011.02.029.
3. V. K. Lakhani, T. K. Pathak, N. H. Vasoya, and K. B. Modi, "Structural parameters and X-ray Debye temperature determination study on copper-ferrite-aluminates," *Solid State Sci.*, vol. 13, no. 3, pp. 539–547, Mar. 2011, doi: 10.1016/J.SOLIDSTATESCIENCES.2010.12.023.
4. V. Tsurkan, H. A. Krug von Nidda, J. Deisenhofer, P. Lunkenheimer, and A. Loidl, "On the complexity of spinels: Magnetic, electronic, and polar ground states," *Phys. Rep.*, vol. 926, pp. 1–86, Sep. 2021, doi: 10.1016/J.PHYSREP.2021.04.002.
5. M. A. Islam *et al.*, "Structural characteristics, cation distribution, and elastic properties of Cr3+ substituted stoichiometric and non-stoichiometric cobalt ferrites," *RSC Adv.*, vol. 12, no. 14, p. 8502, Mar. 2022, doi: 10.1039/D1RA09090A.
6. L. Cornu, M. Duttine, M. Gaudon, and V. Jubera, "Luminescence switch of Mn-Doped ZnAl2O4 powder with temperature," *J. Mater. Chem. C*, vol. 2, no. 44, pp. 9512–9522, Oct. 2014, doi: 10.1039/C4TC01425A.
7. M. U. Rana, Misbah-Ul-Islam, and T. Abbas, "Cation distribution in Cu-substituted manganese ferrites," *Mater. Lett.*, vol. 41, no. 2, pp. 52–56, Oct. 1999, doi: 10.1016/S0167-577X(99)00102-0.
8. D. Yuan, J. Zhao, W. Manalastas, S. Kumar, and M. Srinivasan, "Emerging rechargeable aqueous aluminum ion battery: Status, challenges, and outlooks," *Nano Mater. Sci.*, vol. 2, no. 3, pp. 248–263, Sep. 2020, doi: 10.1016/J.NANOMS.2019.11.001.
9. T. N. Stokes, G. D. Bromiley, G. D. Gatta, N. Rotiroti, N. J. Potts, and K. Saunders, "Cation distribution and valence in synthetic Al–Mn–O and Fe–Mn–O spinels under varying conditions," *Mineral. Mag.*, vol. 82, no. 4, pp. 975–992, Aug. 2018, doi: 10.1180/MGM.2018.109.
10. M. F. Bekheet, L. Schlicker, A. Doran, K. Siemensmeyer, and A. Gurlo, "Ferrimagnetism in manganese-rich gallium and aluminium spinels due to mixed valence Mn2+–Mn3+ states," *Dalt. Trans.*, vol. 47, no. 8, pp. 2727–2738, Feb. 2018, doi: 10.1039/C7DT04765G.
11. A. P. Grosvenor, E. M. Bellhouse, A. Korinek, M. Bugnet, and J. R. Mcdermid, "XPS and EELS Characterization of Mn2SiO4, MnSiO3 and MnAl2O4."
12. A. R. Tanna and H. H. Joshi, "Computer Aided X-Ray Diffraction Intensity Analysis for Spinels: Hands-On Computing Experience," *Int. J. Phys. Math. Sci.*, vol. 7, no. 3, pp. 334–341, Mar. 2013, doi: 10.5281/ZENODO.1333917.
13. S. Wang, X. Wei, H. Gao, and Y. Wei, "Effect of amorphous alumina and α-alumina on optical, color, fluorescence properties and photocatalytic activity of the MnAl2O4 spinel oxides," *Optik (Stuttg).*, vol. 185, pp. 301–310, May 2019, doi: 10.1016/J.IJLEO.2019.03.147.
14. H. Furuhashi, M. Inagaki, and S. Naka, "Determination of cation distribution in spinels by X-ray diffraction method," *J. Inorg. Nucl. Chem.*, vol. 35, no. 8, pp. 3009–3014, Aug. 1973, doi: 10.1016/0022-1902(73)80531-7.

15. M. Edrissi, M. Soleymani, and M. Naderi, "Synthesis of MnAl2O4 nanocrystallites by Pechini and sequential homogenous precipitation methods: Characterization, product comparison, photocatalytic effect, and Taguchi optimization," *J. Sol-Gel Sci. Technol.*, vol. 64, no. 2, pp. 485–492, Nov. 2012, doi: 10.1007/S10971-012-2880-X.
16. A. Shafiekhani and H. Saeidfirozeh, "Influence of Fe@MnAl2O4 and synthesis of novel compound Mn0.83Fe0.21Al1.96O4," *Phys. B Phys. Condens. Matter*, vol. 421, pp. 122–126, 2013, doi: 10.1016/j.physb.2013.04.026.
17. T. O. L. Sunde, T. Grande, and M.-A. Einarsrud, "Modified Pechini Synthesis of Oxide Powders and Thin Films," *Handb. Sol-Gel Sci. Technol.*, pp. 1–30, 2016, doi: 10.1007/978-3-319-19454-7_130-1.
18. B. D. (Bernard D. Cullity, "Elements of x-ray diffraction," p. 555, 1978.
19. D. T. Cromer and J. B. Mann, "X-ray scattering factors computed from numerical Hartree–Fock wave functions," *urn:issn:0567-7394*, vol. 24, no. 2, pp. 321–324, Mar. 1968, doi: 10.1107/S0567739468000550.
20. P. Villars, "MnAl2O4 Crystal Structure," *SpringerMaterials (online database)*, 2016. https://materials.springer.com/isp/crystallographic/docs/sd_1217014.